Available online at www.sciencedirect.com
SCIENCE DIRECT
International Journal of Mass Spectrometry 251 (2006) 138–145
International Journal of Mass Spectrometry
www.elsevier.com/locate/ijms

Decay Q-value of ^{105}Sn and of other nuclei near ^{100}Sn, measured at the GSI on-line mass separator

M. Kavatsyuk [a,b], L. Batist [c], M. Karny [d], E. Roeckl [a,*]

[a] *GSI Darmstadt, Germany*
[b] *National Taras Shevchenko University of Kyiv, Ukraine*
[c] *St. Petersburg Nuclear Physics Institute, Gatchina, Russia*
[d] *Institute of Experimental Physics, Warsaw University, Poland*

Received 30 August 2005; received in revised form 9 January 2006; accepted 11 January 2006
Available online 20 February 2006

Abstract

Within a programme of measuring Q_{EC}, $Q_{EC} - S_p$ and S_p values of nuclei in the ^{100}Sn region, the Q_{EC} value of ^{105}Sn was determined to be 6230 (80) keV. This result was obtained by means of the total-absorption spectrometer at the On-line Mass Separator of GSI Darmstadt. Other decay Q-values of nuclei near ^{100}Sn, measured at this facility by investigating positron, electron-capture, β-delayed proton as well as direct proton and α-decay, are also presented. The accuracy of these data ranges from 30 to 260 keV, is thus lower than that obtained by other methods but still sufficient concerning most of the current nuclear-structure studies. Moreover, the determination of Q-values by means of decay measurements has an unrivalled sensitivity.

Keywords: Binding energies and masses; α, β and proton radioactivity; On-line isotope separation

1. Introduction

In recent years, some of the experimental results on decay Q-values, in particular those based on determining the end-point of a β spectrum, have been shown to deviate from the accurate data obtained by means of Penning traps. In most of the cases, this deviation is apparently due to the fact that the relevant decay work has underestimated the complexity of the decay pattern of heavy nuclei, known as the Pandemonium problem [1]. In principle, the determination of the end-point of a (continuous) β spectrum involves folding a theoretical (potentially multi-component) spectrum with the response function of the detector and fitting the resulting spectrum to the experimental one. This procedure becomes particularly unreliable if the β feedings to particular daughter levels are deduced from high-resolution, low-efficiency spectroscopy of β-delayed γ rays. Even if the entire range of the spectrum is fitted[1] the end-point determination has a high chance of being erroneous as γ-intensity may have been missed by the high-resolution data.

Thus measurements of Q-values by determining the endpoint of β spectra have got a "bad reputation". However, decay Q-values can be determined in a way that avoids the problems mentioned above. We present in this paper experimental data which, we believe, fulfil this quality criterion. They concern decay Q-values and related mass or mass-difference data of nuclei in the ^{100}Sn region. The results were obtained by using the total-absorption spectrometer (TAS) and other decay-spectroscopic devices at the GSI on-line mass separator. The TAS is a high-efficiency, low-resolution device, which is considerably less sensitive to the Pandemonium problem than low-efficiency instruments such as germanium (Ge) detectors. It allows one to directly obtain the β feeding, thus avoiding the problem of missing γ-intensity of (almost all) low-efficiency measurements. More-

* Corresponding author at: GSI Darmstadt, Planckstraße 1, D-64291 Darmstadt, Germany. Fax: +49 6159 712433.
E-mail address: E.Rockl@gsi.de (E. Roeckl).

[1] Fitting only the high-energy part of an experimental β spectrum, notably in the form of a Fermi–Kurie plot, is one of the most common sources of errors in the resulting end-point energy or its uncertainty.

1387-3806/$ – see front matter © 2006 Elsevier B.V. All rights reserved.
doi:10.1016/j.ijms.2006.01.023

over, by detecting characteristic X-rays and positrons (β^+) one can distinguish between the electron-capture (EC) and β^+ component of β-decay. As the ratio between the intensities of the two components for a given β transition depends solely upon the decay energy, the measurement of this quantity offers an excellent method for determining Q-values of β^+/EC transitions. The TAS is thus well suited for measuring, e.g., Q_{EC} and $Q_{EC} - S_p$ values, S_p being the proton separation energy in the β-decay daughter nucleus. The quantity $Q_{EC} - S_p$, energetically characterizing β-delayed proton (βp) decay, is experimentally accessible by detecting protons in the TAS.

After describing TAS including the ancillary detectors and other relevant experimental techniques in Section 2, we shall present a new measurement of the Q_{EC} value of the neutron-deficient isotope ^{105}Sn. This result will be discussed in Section 3 together with those on other Q_{EC} values from TAS-based measurement on nuclei in the ^{100}Sn region, that have already been published elsewhere. This discussion as well as that on Q_{EC} data obtained by other methods will not address nuclear-structure aspects in detail even though they represent the motivation for these studies. Instead we shall put the emphasis on the experimental techniques and shall, e.g., explain why and how different (parts of the) TAS data were used to deduce the Q_{EC} values for the different isotopes of interest and give the main sources of experimental uncertainties. In Section 4 we shall summarise the results and give an outlook to the role of decay Q-value measurements in comparison with mass measurements performed by means of Penning traps and storage rings. While we restrict ourselves to presenting data from the ^{100}Sn region, it should be noted that the TAS has also been used to determine Q_{EC} values of nuclei beyond ^{146}Gd (see e.g., [2]).

2. Experimental techniques used to determine Q_{EC} values

2.1. Sample preparation

The nuclei of interest were produced by fusion–evaporation reactions, stopped in a catcher inside an ion source of the on-line mass separator [3] and released as singly charged ions. After acceleration to 55 keV and mass separation in a dipole magnet, the resulting beam was implanted into a tape, which was operated in two different modes. Firstly, it was positioned in the centre of an array of charged-particle and γ ray detectors and was regularly removed from the measuring position in order to avoid build-up of long-lived daughter activities. In the recent measurements discussed here, three silicon-strip detectors were used for the former and 17 Ge crystals for the latter purpose. Secondly, the mass-separated beam of interest was collected on the tape for a pre-selected time interval, the resulting activity was then moved into the centre of the TAS where it remained during the measuring interval. As an alternative to the moving-tape collector, the mass-separated beam was implanted into a thin foil viewed by a silicon-detector telescope, with the beam being switched on and off in order to allow a half-life analysis. The latter device was used for α spectroscopy. In all three-operation modes, many collection, collection-counting or collection-decay cycles were repeated until sufficient statistics was reached.

2.2. Total absorption spectrometer

The main part of the TAS [4] is a single NaI crystal with a cylindrical well in its center, permitting the installation of auxiliary detectors and the insertion of the radioactive sources via the tape transport system. The device is well suited detecting the whole γ cascade following β^+, EC or βp processes. The auxiliary detectors such as silicon (Si) and Ge detectors serve for distinguishing between these different disintegration modes. The tape was viewed by two 0.5 mm thick Si detectors. One of them, abbreviated as "BOT Si", viewed the tape from the "bottom" side where the ions had been implanted. The other one, abbreviated as "TOP Si", was mounted at the opposite, i.e., "top" side of the tape. Both Si detectors were used to detect positrons and protons. In the case of the "TOP Si" detector the protons suffered a major energy loss as they had to pass the tape. By demanding coincidence between the two Si detectors we were able to identify β^+-related pβ events (β^+p). Close to the TOP Si detector, a 2 cm^3 Ge crystal, equipped with a thin beryllium window, was mounted which was used to measure β^+ spectra or to identify EC decay by recording characteristic X-rays. Separate TAS measurements with longer collection-counting intervals were performed in order to determine the isobaric contamination and to perform the corresponding correction of the experimental data.

2.3. Determining Q_{EC} values from the endpoint of a β^+ spectrum

As mentioned above, the determination of the endpoint of an experimental β spectrum from a fit to a theoretical one is a laborious procedure in case of the decay of heavy nuclei. Nevertheless this method, abbreviated by the acronym "β^+ spectrum" in the following, has been used to determine the Q_{EC} value of an isomer of ^{70}Br [5]. This experiment is characterised by the following two quality criteria, which are not fulfilled by most endpoint measurements. Firstly, by using the TAS one and only one β-decay branch of the isomer was selected. This is an important prerequisite for an endpoint-determination of a β disintegration of a heavy nucleus, which generally has many components corresponding to the population of different states in the daughter nucleus. Secondly, the one-component β^+ spectrum obtained in this way was compared to a theoretical one, folded with the response function of the Ge detector, in a fit that extended over almost the entire range of the experimental spectrum.

2.4. Determining Q_{EC} values from EC/β^+ ratios of β-decay

The ratio of EC and β^+ intensities (I_{EC}/I_{β^+}) plotted as a function of the excitation energy of the β-decay daughter nucleus depends only on the Q_{EC} value. In order to experimentally deduce the latter quantity, the TAS is used to select β transitions or to measure the (entire) distribution of the EC and β^+-intensity as a function of the excitation energy of the

β-decay daughter nucleus. The excitation-energy dependent, experimental I_{EC}/I_{β^+} ratio, properly corrected for the relevant TAS efficiencies, is fitted by the corresponding theoretical I_{EC}/I_{β^+} values, with the Q_{EC} value being the only free parameter in a χ^2 minimisation procedure. This method, which will be characterised by the acronym "EC/β+", requires a sufficiently large EC decay component of the β-decay considered and hence works best for high atomic number and not too high Q_{EC} values, i.e., for mean-mass or heavy nuclei not too far from stability.

2.5. Determining $Q_{EC} - S_p$ values from the EC/β+ ratios of β-delayed proton decay

The decay Q-value of βp emission, $Q_{EC} - S_p$, can be determined by a method similar to that described in Section 2.4, except that the ratio of the EC-delayed and β+-delayed proton intensity (I_{ECp}/I_{β^+p}) is considered as function of the energy of the protons emitted. The $Q_{EC} - S_p$ value is the only free parameter in fitting the experimental I_{ECp}/I_{β^+p} distribution to theoretical one. This method will be characterised by the acronym ECp/β+p. If S_p is known the Q_{EC} value can be deduced. If, on the other hand, the Q_{EC} value is known, the ECp/β+p method yields S_p. This method requires a sizable branching ratio for β-delayed proton emission and is hence suitable for nuclei very far from stability.

3. Results and discussion

3.1. Determination of the Q_{EC} value of ^{105}Sn

^{105}Sn has recently been studied by means of in-beam and β-decay spectroscopy [6–11]. Such measurements allow one to study high-spin levels in ^{105}Sn and (low-spin) states in the β-decay daughter, ^{105}In, respectively. Previous β-decay work included measurements of β-delayed γ rays [12,13] and protons [14], yielding a half-life of 34 s for ^{105}Sn [13] and evidence for a 1/2−, 48 s isomer in ^{105}In at an excitation energy of 674 keV [15]. However, the Q_{EC} value of ^{105}Sn was not directly measured so far, but inferred from a "mass loop" involving the known mass excess of ^{108}Sn and the α-decay energy as well as the $Q_{EC} - S_p$ value of ^{109}Te [13].

^{105}Sn was produced in the fusion–evaporation reaction ^{50}Cr(^{58}Ni, 1n2p). A 5.2 MeV/u ^{58}Ni beam of about 40 particle-nA from the linear accelerator UNILAC impinged on an enriched ^{50}Cr target (4 mg/cm^2, enrichment 97%). A FEBIAD-B3C ion source with ZrO_2 catcher was used. High chemical selectivity for tin was achieved by adding CS_2 vapour to the ion source. Using this technique about 60% of the ^{105}Sn ion-output is shifted to the ^{105}Sn^{32}S$^+$ molecular side-band, thus suppressing strongly the isobaric contaminants, i.e., ^{105}In, ^{105}Cd, ^{105}Ag, and ^{105}Pd [16]. After ionisation, acceleration to 55 keV and mass separation in a magnetic sector field, the $A = 105 + 32$ ions were delivered to the TAS (see Sections 2.1 and 2.2).

Taking into account the half-life of ^{105}Sn and those of the contaminants, the cycle of the transport tape (see Section 2.1) was chosen to have a collection period of 32 s and a counting period of 64 s. In this way the activity of ^{105}Sn was favoured and that of the contaminants was suppressed. In order to be able to correct the data for contributions from contaminants, the latter were measured in separate experiments with collection/counting periods of 32/256, 64/256 and 64/512 s, respectively. The total measurement time used to take $A = 105 + 32$ data amounted to 8 h for the main experiment on the ^{105}Sn decay and 5.5 h for measuring contributions from contaminants.

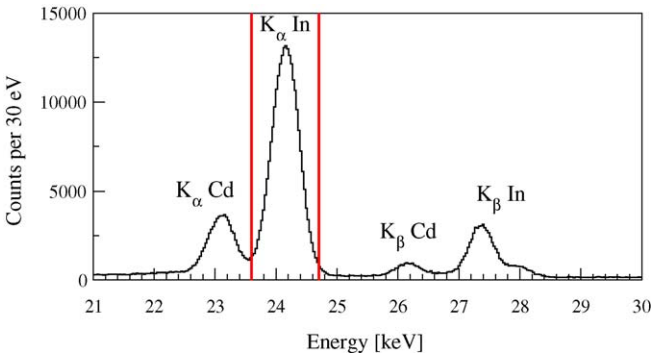

Fig. 1. Spectrum of X-rays registered by the Ge detector of the TAS during the $A = 105 + 32$ measurement. The data were obtained by demanding coincidence with the NaI crystal and anticoincidence with the Si detectors. These conditions reduce the probability of recording γ rays, positrons, conversion electrons in the Ge detector. Vertical lines indicate the gate used for selecting indium K$_\alpha$ X-rays and thus the EC component of the ^{105}Sn decay.

The TAS spectrum corresponding to the EC decay component of ^{105}Sn (TAS (EC)) can be obtained by detecting γ rays in the NaI crystal in coincidence with characteristic indium X-rays registered in Ge detector. The relevant X-ray spectrum and gate condition are shown in Fig. 1. In order to estimate the contribution of electron conversion of ^{105}In transitions, we searched for conversion electrons occurring in the ^{105}Sn decay. This was done by inspecting the BOT Si spectrum accumulated by demanding coincidence with the above-mentioned indium X-ray gate This spectrum, displayed in Fig. 2, shows a peak at about 650 keV which is interpreted as being due to conversion electrons emitted in the 674 keV transition de-exciting the 1/2− isomer in ^{105}In, which is known to get a sizable feeding in the decay of ^{105}Sn (Kavatsyuk et al., to be published). However, the isomer has a

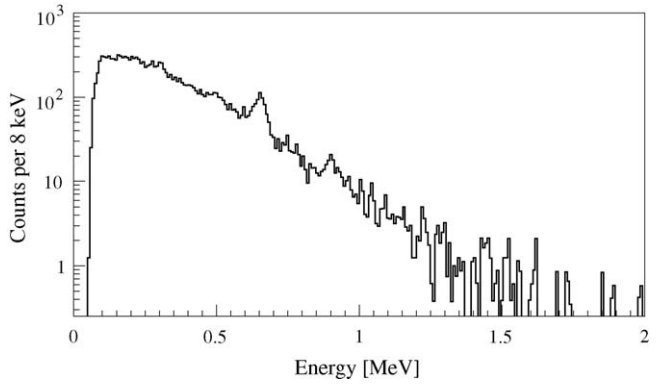

Fig. 2. Spectra measured by the BOT Si detectors for mass $A = 105 + 32$. The data were obtained by demanding coincidence with indium X-rays recorded by the Ge detector.

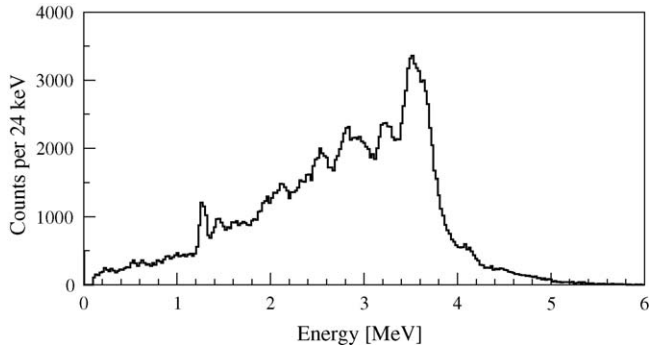

Fig. 3. TAS spectrum representing the EC component of the ^{105}Sn decay.

long half-life and the 650 keV line can thus be disregarded in the search for promptly emitted conversion electrons discussed here. Considering the structure occurring at about 900 keV in Fig. 2 to indicate a potential conversion-electron line we deduced an upper limit of about 4×10^{-3} per ^{105}Sn decay for the corresponding β-intensity. This together with the positron-detection efficiency of 82% [17] of the BOT and TOP Si detectors, used for setting the anticoincidence condition when accumulating the spectrum shown in Fig. 1, yield an upper limit of about 10^{-3} per ^{105}Sn decay for a corresponding conversion-electron contributions to the indium K_α peak and thus to the corresponding gate (see Fig. 1) used for generating the TAS (EC) spectrum. Therefore, the TAS (EC) spectrum displayed in Fig. 3 contains an equally small admixture of conversion electron contributions, which was neglected in the following evaluation.

To select the β^+ component of the ^{105}Sn decay (TAS (β^+)), coincidences were demanded between signals from the NaI crystal and positrons registered in the BOT Si or TOP Si detectors. Figs. 4 and 5 show the spectra accumulated in the latter two detectors and the corresponding TAS (β^+) spectrum, respectively. However, in the case of selection of the β^+ decay component, the TAS (β^+) spectrum resulting from applying the positron gate had to be corrected for contributions from contaminants, as described in the Ref. [17]. The resulting background-free TAS (β^+) spectrum is shown in Fig. 5.

In order to determine the β-intensity distributions for EC and β^+ decay of the ^{105}Sn, a set of TAS spectra corresponding to the

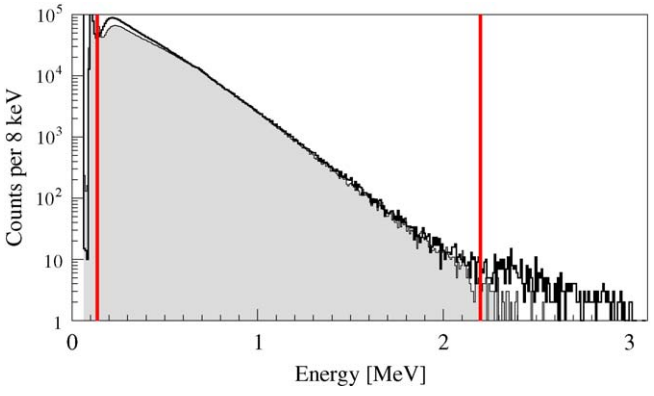

Fig. 4. Spectra measured by the TOP Si (shaded-area histogram) and BOT Si (black-line histogram) detectors for mass $A = 105 + 32$. Vertical lines indicate gate used for selecting β^+ component of the decay.

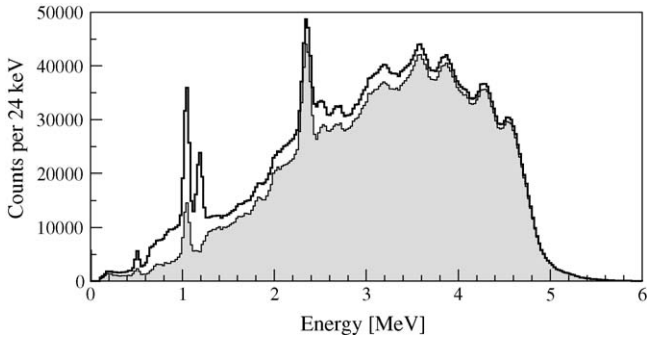

Fig. 5. TAS spectrum of the β^+ component obtained for $A = 105 + 32$ by gating on the Si TOP and Si BOT detectors (black-line histogram). The TAS spectrum corresponding to the β^+ decay of the ^{105}Sn decay (shaded-area histogram) was generated after subtracting of the isobaric contaminants.

population of selected ^{105}In levels has to be assumed and fitted to the experimental TAS (EC) and/or TAS (β^+) spectra, with the β-intensities of these levels being variable parameters. The simulations were performed by using the Monte–Carlo tool kit GEANT-4 [18] and the information on the $^{105}\text{Sn} \rightarrow {}^{105}$In decay scheme from the previous work [13]. As the latter data did not yield a satisfactory fit to the TAS spectra, β feeding of additional excitation-energy intervals in ^{105}In had to be introduced (Kavatsyuk et al., to be published). Details on this procedure are given in Ref. [17]. During the simulation, γ-feeding of the $1/2^-$ isomer in ^{105}In was taken into account. To determine the Q_{EC} value of the ^{105}Sn decay, the TAS (EC) and TAS (β^+) spectra were evaluated separately, yielding the two β-intensity distributions (I_{EC}, I_{β^+}) shown in Fig. 6. The intensity scales of the I_{EC} and I_{β^+} spectra were determined to reproduce a value of 0.420 (35) for the EC contribution to the ^{105}Sn decay. The latter result was obtained from the areas of the TAS (EC) and TAS (β^+) spectra, taking the gate efficiencies into account (Kavatsyuk et al., to be published). The I_{EC} and I_{β^+} distributions, displayed in Fig. 6, were used to deduce the dependence of the I_{EC}/I_{β^+} ratio

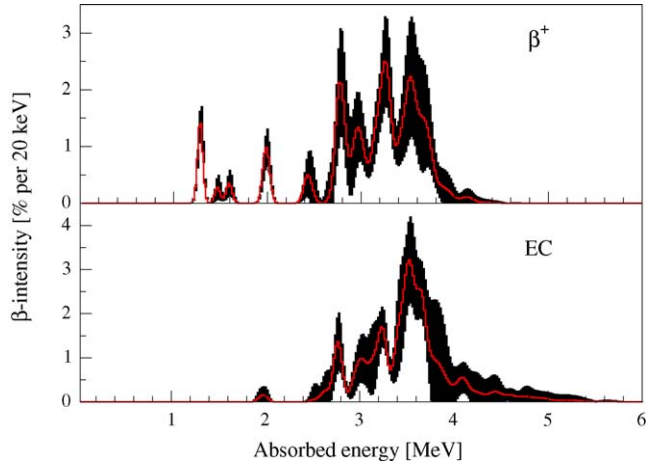

Fig. 6. Beta-intensity distributions obtained from independent analyses of the TAS (EC) and TAS (β^+) spectra of ^{105}Sn. The distributions shown in black are the experimental ones, with the hatched areas indicating the uncertainties. The light grey curves represent the results of simulations. All spectra were normalised to 100% disregarding the experimentally determined EC/β^+ ratio (see text).

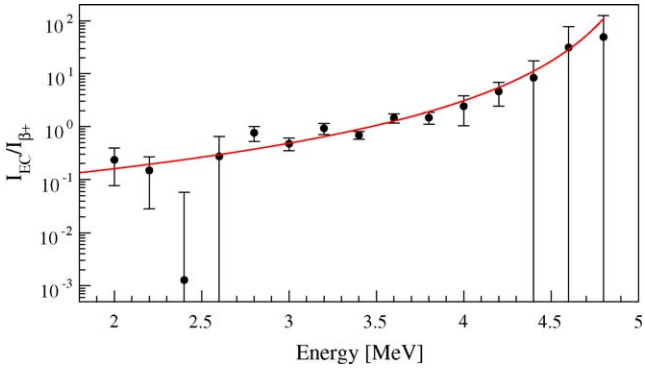

Fig. 7. Ratio of EC and β^+ intensities ^{105}Sn as a function of the ^{105}In excitation-energy from experiment (full circles with uncertainties) and from a fit that is based on theoretical EC and β^+ intensities (curve) and yields a Q_{EC} value of 6230 (80) keV.

upon ^{105}In excitation energy, shown in Fig. 7. The I_{EC}/I_{β^+} values were averaged over excitation-energy intervals of 200 keV in order to have sufficient statistics in each energy interval. By using the theoretical $f_{EC}(Q_{EC} - E)/f_{\beta^+}(Q_{EC} - E)$ ratios [19], the normalised I_{EC}/I_{β^+} data were fitted, with the Q_{EC} value of ^{105}Sn being the only free parameter, where E is the excitation energy of daughter nucleus and $f(E)$ the statistical rate function. The fitting procedure yielded a Q_{EC} value of 6230 (80) keV for ^{105}Sn. Details on the distribution of the total β-intensity and of the Gamow–Teller strength of ^{105}Sn, deduced from the TAS data, will be discussed elsewhere (Kavatsyuk et al., to be published).

3.2. Discussion of Q_{EC} values of nuclei in the ^{100}Sn region, obtained from TAS measurements

The experimental Q_{EC} value of ^{105}Sn, determined in this work, and other Q_{EC}, $Q_{EC} - S_p$ and S_p values obtained by TAS measurements are listed in Table 1. The data compiled in Table 1 represent cases where the measurement either yielded the respective mass data for the first time or considerably improved their accuracy. The only exceptions are ^{103}In and ^{105}Sn where the TAS-based results of 6040 (60) and 6230 (80) keV were of comparable accuracy as the previous values of 6050 (20) [28] and 6220 (80) keV [13], respectively. As already mentioned in Section 3.1, the latter result used a mass loop between the mass excess of ^{108}Sn and the α-decay energy as well as the $Q_{EC} - S_p$ value of ^{109}Te [13]. The Q_{EC} value of ^{105}Sn, presented in this work, confirms the mass and Q-values that were used in the loop procedure. The TAS work on $^{104–107}$In [29] is not included in Table 1, as in this case Q_{EC} data from the literature [30] served to deduce the Gamow–Teller strength distributions.

In the following discussion of the data presented in Table 1, particular emphasis will be put on experimental parameters such as accuracy. For the physics motivation of the corresponding experiments, which are related to investigating isomers [5,20], the Gamow–Teller strength distribution [17,20–25], lifetimes of proton-emitting levels [26] or other properties of excited levels [26,27], the reader is referred to the published literature.

The following statements can be made concerning data listed in Table 1:

- The experimental accuracy from 60 to 260 keV was sufficient for meeting the physics requirements of the various works.
- The Q_{EC} values can be used to determine the mass of the parent nucleus, provided the mass of the daughter nucleus is known. Assuming that the mass of the latter quantity is known with better accuracy than the former, which is generally the case, the relative accuracy of such mass determinations is of the order 10^{-6} for the cases compiled in Table 1.
- The sensitivity of TAS-based determinations of Q_{EC} and $Q_{EC} - S_p$ can be demonstrated by the example of ^{100}In. An accuracy of 130 and 230 keV, respectively, was obtained by using a ^{100}In beam intensity of 2 atoms/s during a measuring time of 90 h [22].

Table 1
Compilation of Q_{EC}, $Q_{EC} - S_p$ and S_p values obtained by using TAS

Parent nucleus	Q_{EC} value (keV)	$Q_{EC} - S_p$ (keV)	S_p (keV)	Method	Reference
^{70m}Br	$12190 \pm 70_{sta} \pm 40_{sys}$			β^+ spectrum	Karny et al. [5]
^{96}Ag	11660 (240)[a]	6430 (60)		ECp/β^+p	Batist et al. [20]
^{97}Ag	6980 (110)			EC/β^+	Hu et al. [21]
^{98}Ag	8200 (70)			EC/β^+	Hu et al. [22]
^{100}In	10080 (230)[b]	5250 (130)		ECp/β^+p	Plettner et al. [23]
^{102}In	8950 (120)			EC/β^+	Gierlik et al. [24]
^{103}In	6040 (60)			EC/β^+	Karny et al. [25]
^{103}Sn	7640 (70)[c]	5400 (100)		EC/β^+, ECp/β^+p	Kavatsyuk et al. [17]
^{105}Sn	6230 (80)			EC/total	This work
^{113}Xe		8300 (150)	690 (60)[d]	ECp/β^+p	Janas et al. [26]
^{117}Ba	8990 (260)[e]	8300 (250)		ECp/β^+p	Janas et al. [27]

See text for details.

[a] Result obtained by using the known S_p value of ^{96}Pd and data on isomerism in this nucleus [20].

[b] Result obtained by using the known S_p value of ^{100}Cd [23].

[c] Weighted average between the value of 7660 (100) keV obtained by the EC/β^+ method and the value of 7610 (110) keV obtained by the combining the ($Q_{EC} - S_p$) result with the known S_p value of ^{103}In [17].

[d] Result obtained by using the known Q_{EC} value of ^{113}Xe [26].

[e] Result obtained by using the known S_p value of ^{117}Cs [27].

- Some of the data given in Table 1 are limited in accuracy, simply because the measuring time of the related experiments were too short. These results could easily be improved by extending the counting time.

3.3. Determination of decay Q-values by other methods

We shall discuss three examples of direct charged particle radioactivity of nuclei beyond ^{100}Sn here, which allow one to deduce decay Q-values, masses and separation energies. The examples are taken again from work performed at the GSI on-line mass separator, putting emphasis again on mass measurements, their accuracy and sensitivity rather than on the other underlying physics motivations, which are described in detail in Refs. [31–33].

Firstly, the three α-decays in the chain ^{114}Ba → ^{110}Xe → ^{106}Te → ^{102}Sn [31] do not only yield information on three important mass differences of nuclei above ^{100}Sn, hence on the mass surface in this region of the chart of nuclides, but also on the Q-value for ^{12}C decay of ^{114}Ba, the latter decay mode being unobserved for such nuclei to date. The intensity of the mass-separated ^{114}Ba beam amounted to 4 atoms/min, which due to the branching ratio of about 0.9% for α-decay of this isotope, corresponds to a partial beam intensity of 2 atoms/h. During a measuring time of 56 h the α-decay Q-value of ^{114}Ba was determined with an accuracy of 40 keV.

Secondly, the study of direct proton radioactivity of the (21$^+$) isomer of ^{94}Ag [32] has shown that the Q-value for this decay, with respect to the ground-state of the daughter nucleus ^{93}Rh, is 5780 (30) keV. Combining this result with the value of 890 (500) keV [34], extrapolated from systematic trends for the proton separation energy of ^{94}Ag, the excitation energy of this isomer was estimated to be 6700 (500) keV. The intensity of the mass-separated beam of the (21$^+$) isomer of ^{94}Ag amounted to 10 atoms/min. As the branching ratio for each of the two proton lines was found to be about 2/100 decays, they were observed at a partial beam intensity of 15 atoms/h. A measurement time of 80 h was sufficient to reach a Q-value accuracy of 30 keV.

Thirdly, the observation of two-proton decay of the (21$^+$) isomer [33] has yielded the proton separation energy in ^{93}Rh to be 2330 (100) keV. This corresponds to a 2σ deviation from the value of 3630 (570) keV extrapolated from systematic trends [34]. Based on the above-mentioned intensity data for the direct proton radioactivity of the (21$^+$) isomer of ^{94}Ag, the branching ratio of 5/1000 decays found for the two-proton emission corresponds to a partial beam intensity of 3 atoms/h for this decay mode of the isomer.

4. Summary and conclusion

We have described the measurement of the Q_{EC} value of ^{105}Sn and discussed this result together with other mass-differences determined for nuclei in the ^{100}Sn region. All data have been obtained by using the TAS or other decay-spectroscopic devices at the GSI on-line mass separator. The relative accuracy of the mass measurements is of the order of 10^{-6}. This is sufficient for the physics aims of the corresponding experiments, which include the determination of (i) the excitation energy of isomers, (ii) the Gamow–Teller strength distribution, (iii) lifetime of proton-emitting levels, and (iv) other properties of excited states allowing one to check statistical-model calculations. Moreover, the accuracy is sufficient for testing theoretical predictions of atomic masses.

In view of the remarkable success of mass measurements based on Penning traps and storage rings it lies close at hand to predict that they will be the one and only method used for determining nuclear masses and decay Q-values in the future. In this context, it is interesting to compare the level of Q-value or mass accuracy as well as the sensitivity reached by Q-value experiments with the corresponding data from Penning-trap measurements, taking the cases of ^{22}Mg [35], ^{32}Ar, ^{33}Ar [36], ^{72}Kr [37], ^{74}Kr and ^{74}Rb [38] as examples. In these experiments, the mass-excess values were obtained with uncertainties between 0.27 and 4 keV, corresponding to relative uncertainties of 1.4×10^{-8} and 1.2×10^{-7}. On the one hand, the precision achieved by trap measurements and required for the physics cases underlying these studies is one to two orders of magnitude higher than that reached in the above-mentioned Q-value measurements. The latter data, however, are of sufficient accuracy for meeting the requirements of the corresponding physics aims. On the other hand, such Penning-trap measurements require intensities of atleast 100 atoms/s [39]. This level is two orders of magnitude higher than that of Q_{EC} determinations and some five orders of magnitude orders higher than that of experiments based on detecting proton or α radioactivity. In addition to the intensity of the radioactive beam of interest, its purity is a key quantity. For Penning-trap measurements the intensity of isobaric contaminants, including atoms or molecules of stable isotopes, should not be higher than 10^3 times that of the wanted species (Herfurth, Private communication). Decay measurements on mass-separated beams apparently suffer less from isobaric contamination, in particular if they involve detection of protons or α particles. The considerations described in this paragraph represent a snapshot of the experimental situation today and do not take the potential of future improvements into account.

All in all, for the time being decay spectroscopy is a valuable technique for measuring masses of nuclei very far from stability, including in particular nuclei beyond the proton drip line, and it seems as if it will continue to be one of the key methods of future nuclear-physics research. Due to its high sensitive, it is well suited for studying the most exotic nuclei, which are produced at very low rates, including their decay Q-values and masses. Moreover, decay studies yield information beyond the mass, namely detailed data on transitions mediated by the electromagnetic, weak and strong interaction. The advantages of ion traps and the attractive features of decay spectroscopy have recently lead to combining them into what was recently baptised “trap-assisted decay spectroscopy” [40]. We hope that the results presented in this work are of interest to those intending to use this novel spectroscopic tool.

Acknowledgements

This work was supported in part by the Polish Committee of Scientific Research, in particular under Grant no. KBN 2 P03B 035 23. In spite of hating pompous birthday addresses, one of the authors (E.R.) would like to acknowledge 35 years of numerous friendly-collaborative encounters with Jürgen Kluge, 65 years of age now, which took place inside and outside various laboratories and ranged from meeting at ISOLDE through jointly lecturing at Mainz University and doing research at GSI all the way to today's enjoyable neighbourhood within GSI's Atomic Physics Division: Ad multos annos!

References

[1] J.C. Hardy, L.C. Carraz, B. Jonson, P.G. Hansen, Phys. Lett. B. 71 (1977) 307.
[2] A. Algora, L. Batist, M.J.G. Borge, D. Cano-Ott, R. Collatz, S. Courtin, Ph. Dessagne, L.M. Fraile, A. Gadea, W. Gelletly, M. Hellström, Z. Janas, A. Jungclaus, M. Karny, R. Kirchner, G. Le Scornet, F. Maréchal, Ch. Miehé, F. Moroz, E. Nácher, E. Poirier, E. Roeckl, B. Rubio, K. Rykaczewski, J.L. Tain, O. Tengblad, V. Wittman, Eur. Phys. J. A 20 (2004) 199.
[3] E. Roeckl, A. Blazhev, K. Burkard, J. Döring, H. Grawe, W. Hüller, R. Kirchner, C. Mazzocchi, I. Mukha, C. Plettner, Nucl. Instrum. Methods Phys. Res. B 204 (2003) 53.
[4] M. Karny, J.M. Nitschke, L.F. Archambault, K. Burkard, D. Cano-Ott, M. Hellström, W. Hueller, R. Kirchner, S. Lewandowski, E. Roeckl, A. Sulik, Nucl. Instrum. Methods Phys. Res. B 126 (1997) 411.
[5] M. Karny, L. Batist, D. Jenkins, M. Kavatsyuk, O. Kavatsyuk, R. Kirchner, A. Korgul, E. Roeckl, J. Żylicz, Phys. Rev. C 70 (2004) 014310-1.
[6] K. Deneffe, E. Coenen, M. Huyse, P. Van Duppen, J. Vanhorenbeek, P. del Marmol, P. Fettweis, J. Phys. G 11 (1985) L59.
[7] R. Schubart, H. Grawe, J. Heese, H. Kluge, K.H. Maier, M. Schramm, J. Grebosz, L. Käubler, H. Rotter, J. Kownacki, D. Seweryniak, Z. Phys. A 343 (1992) 123.
[8] G. de Angelis, E. Farnea, A. Gadea, M. Sferrazza, D. Ackermann, D. Bazzacco, P. Bednarczyk, P.G. Bizzeti, A.M. Bizzeti Sona, F. Brandolini, R. Burch, A. Buscemi, D. De Acuna, M. De Poli, C. Fahlander, Y. Li, M. Lipoglavsek, S. Lunardi, A. Makishima, R. Menegazzo, L. Muller, D. Napoli, M. Ogawa, P. Pavan, C. Rossi-Alvarez, F. Scarlassara, G.F. Segato, D. Seweryniak, F. Soramel, P. Spolaore, R. Zanon, the NORDBALL Collaboration, Nucl. Phys. A 583 (1995) 231c.
[9] A. Gadea, G. de Angelis, C. Fahlander, M. De Poli, E. Farnea, Y. Li, D.R. Napoli, Q. Pan, P. Spolaore, D. Bazzacco, S.M. Lenzi, S. Lunardi, C.M. Petrache, F. Brandolini, P. Pavan, C. Rossi Alvarez, M. Sferrazza, P.G. Bizzeti, A.M. Bizzeti Sona, J. Nyberg, M. Lipoglavsek, J. Persson, J. Cederkäll, D. Seweryniak, A. Johnson, H. Grawe, F. Soramel, M. Ogawa, A. Makishima, R. Schubart, S. Frauendorf, Phys. Rev. C 55 (1997) R1.
[10] A. Gadea, G. de Angelis, C. Fahlander, M. De Poli, E. Farnea, Y. Li, D.R. Napoli, Q. Pan, P. Spolaore, D. Bazzacco, S.M. Lenzi, S. Lunardi, C.M. Petrache, F. Brandolini, P. Pavan, C. Rossi Alvarez, M. Sferrazza, P.G. Bizzeti, A.M. Bizzeti Sona, J. Nyberg, M. Lipoglavsek, J. Persson, J. Cederkäll, D. Seweryniak, A. Johnson, H. Grawe, F. Soramel, M. Ogawa, A. Makishima, R. Schubart, S. Frauendorf, Z. Phys. A 358 (1997) 193.
[11] G. de Angelis, N. Belcari, D. De Acufia, D.R. Napoli, T. Martinez, M. De Poli, P. Spolaore, G. Prete, E. Fioretto, P. Bednarczyk, A. Gadea, E. Farnea, C.A. Ur, D. Bazzacco, S.M. Lenzi, S. Lunardi, P. Pavan, C. Rossi Alvarez, F. Soramel, P.G. Bizzeti, A.M. Bizzeti-Sona, H. Grawe, R. Schubart, A. Johnson, R. Wyss, F. Xug, N. Blasi, G. Lo Bianco, J. Nyberg, J. Persson, C. Fahlander, D. Rudolph, S. Frauendorf, Nucl. Phys. A (Suppl.) 654 (1999) 659c.
[12] M. Huyse, G. Brijs, P. de Bisschop, J. Gentens, E. Coenen, K. Deneffe, P. Van Duppen, Hyperfine Interact. 22 (1985) 439.
[13] M. Pfützner, A. Płochocki, K. Rykaczewski, J. Szerypo, J. Żylicz, H. Keller, R. Kirchner, O. Klepper, E. Roeckl, D. Schardt, M. Huyse, G. Reusen, P. Van Duppen, B.A. Brown, Nucl. Phys. A 581 (1995) 205.
[14] P. Tidemand-Petersson, R. Kirchner, O. Klepper, W. Kurcewicz, E. Roeckl, E.F. Zganjar, Z. Phys. A 302 (1981) 343.
[15] D. De Frenne, E. Jacobs, Nucl. Data Sheets 68 (1993) 935.
[16] R. Kirchner, Nucl. Instrum. Methods B 204 (2003) 179.
[17] O. Kavatsyuk, O. Kavatsyuk, L. Batist, A. Banu, F. Becker, A. Blazhev, W. Brüchle, K. Burkard, J. Döring, T. Faestermann, M. Górska, H. Grawe, Z. Janas, A. Jungclaus, M. Karny, R. Kirchner, M. La Commara, S. Mandal, C. Mazzocchi, I. Mukha, S. Muralithar, C. Plettner, A. Płochocki, E. Roeckl, M. Romoli, M. Schädel, R. Schwengner, J. Żylicz, Eur. Phys. J. A 25 (2005) 211.
[18] S. Agostinelli, J. Allison, K. Amako, J. Apostolakis, H. Araujoa, P. Arce, M. Asai, D. Axen, S. Banerjee, G. Barrand, F. Behner, L. Bellagamba, J. Boudreau, L. Broglia, A. Brunengo, H. Burkhardt, S. Chauvieb, J. Chuma, R. Chytracek, G. Cooperman, G. Cosm, P. Degtyarenko, A. Dell'Acqua, G. Depaola, D. Dietrich, R. Enamia, A. Feliciello, C. Ferguson, H. Fesefeldt, G. Folger, F. Foppiano, A. Forti, S. Garelli, S. Giani, R. Giannitrapani, D. Gibin, J.J. Gómez Cadenas, I. González, G. Gracia Abril, G. Greeniaus, W. Greiner, V. Grichin, A. Grossheim, S. Guatelli, P. Gumplinger, R. Hamatsu, K. Hashimoto, H. Hasui, A. Heikkinen, A. Howard, V. Ivanchenko, A. Johnson, F.W. Jones, J. Kallenbach, N. Kanaya, M. Kawabata, Y. Kawabata, M. Kawaguti, S. Kelner, P. Kent, A. Kimura, T. Kodama, R. Kokoulin, M. Kossov, H. Kurashige, E. Lamanna, T. Lampén, V. Lara, V. Lefebure, F. Lei, M. Liendl, W. Lockman, F. Longo, S. Magni, M. Maire, E. Medernach, K. Minamimoto, P. Mora de Freitas, Y. Morita, K. Murakami, M. Nagamatua, R. Nartallo, P. Nieminen, T. Nishimura, K. Ohtsubo, M. Okamura, S. O'Neale, Y. Oohata, K. Paech, J. Perl, A. Pfeiffer, M.G. Pia, F. Ranjard, A. Rybin, S. Sadilov, E. Di Salvo, G. Santin, T. Sasaki, N. Savvas, Y. Sawada, S. Scherer, S. Sei, V. Sirotenko, D. Smith, N. Starkov, H. Stoecker, J. Sulkimo, M. Takahata, S. Tanaka, E. Tcherniaev, E. Safai Tehrani, M. Tropeano, P. Truscott, H. Uno, L. Urban, P. Urban, M. Verderi, A. Walkden, W. Wander, H. Weber, J.P. Wellisch, T. Wenaus, D.C. Williams, D. Wright, T. Yamada, H. Yoshida, D. Zschiesche, Nucl. Instrum. Methods A 506 (2003) 250.
[19] N.B. Gove, M.J. Martin, Nucl. Data Tables A 10 (1968) 205.
[20] L. Batist, J. Döring, I. Mukha, C. Plettner, C.R. Bingham, R. Borcea, M. Gierlik, H. Grawe, K. Hauschild, Z. Janas, I.P. Johnstone, M. Karny, M. Kavatsyuk, R. Kirchner, M. La Commara, C. Mazzocchi, F. Moroz, J. Pavan, A. Płochocki, E. Roeckl, B. Salvachúa, K. Schmidt, R. Schwengner, L.D. Skouras, S.L. Tabor, M. Wiedeking, Nucl. Phys. A 720 (2003) 245.
[21] Z. Hu, L. Batist, J. Agramunt, A. Algora, B.A. Brown, D. Cano-Ott, R. Collatz, A. Gadea, M. Gierlik, M. Górska, H. Grawe, M. Hellström, Z. Janas, M. Karny, R. Kirchner, F. Moroz, A. Płochocki, M. Rejmund, E. Roeckl, B. Rubio, M. Shibata, J. Szerypo, J.L. Tain, V. Wittmann, Phys. Rev. C 60 (1999) 024315-1.
[22] Z. Hu, L. Batist, J. Agramunt, A. Algora, B.A. Brown, D. Cano-Ott, R. Collatz, A. Gadea, M. Gierlik, M. Górska, H. Grawe, M. Hellström, Z. Janas, M. Karny, R. Kirchner, F. Moroz, A. Płochocki, M. Rejmund, E. Roeckl, B. Rubio, M. Shibata, J. Szerypo, J.L. Tain, V. Wittmann, Phys. Rev. C 62 (2000) 064315-1.
[23] C. Plettner, L. Batist, J. Döring, A. Blazhev, H. Grawe, V. Belleguic, C.R. Bingham, R. Borcea, M. Gierlik, M. Górska, N. Harrington, Z. Janas, M. Karny, R. Kirchner, C. Mazzocchi, P. Munro, E. Roeckl, K. Schmidt, R. Schwengner, Phys. Rev. C 66 (2002) 044319-1.
[24] M. Gierlik, A. Płochocki, M. Karny, W. Urban, Z. Janas, L. Batist, F. Moroz, R. Collatz, M. Górska, H. Grawe, M. Hellström, Z. Hu, R. Kirchner, W. Liu, M. Rejmund, E. Roeckl, M. Shibata, J. Agramunt, A. Algora, A. Gadea, B. Rubio, J.L. Tain, D. Cano-Ott, S. Harissopoulos, Nucl. Phys. A 724 (2003) 313.
[25] M. Karny, L. Batist, B.A. Brown, D. Cano-Ott, R. Collatz, A. Gadea, R. Grzywacz, A. Guglielmetti, M. Hellström, Z. Hu, Z. Janas, R. Kirchner, F. Moroz, A. Piechaczek, A. Płochocki, E. Roeckl, B. Rubio, K.

Rykaczewski, M. Shibata, J. Szerypo, J.L. Tain, V. Wittmann, A. Wöhr, Nucl. Phys. A 640 (1998) 3.
[26] Z. Janas, L. Batist, R. Borcea, J. Döring, M. Gierlik, M. Karny, R. Kirchner, M. La Commara, S. Mandal, C. Mazzocchi, F. Moroz, S. Orlov, A. Płochocki, E. Roeckl, J. Żylicz, Eur. Phys. J. A 24 (2005) 205.
[27] Z. Janas, L. Batist, J. Döring, M. Gierlik, R. Kirchner, J. Kurcewicz, H. Mahmud, C. Mazzocchi, A. Płochocki, E. Roeckl, K. Schmidt, P.J. Woods, J. Żylicz, Eur. Phys. J. A 23 (2005) 401.
[28] V.R. Bom, R.W. Hollander, E. Coenen, K. Deneffe, P. Van Duppen, M. Huyse, Z. Phys. A 331 (1988) 21.
[29] M. Karny, L. Batist, B.A. Brown, D. Cano-Ott, R. Collatz, A. Gadea, R. Grzywacz, A. Guglielmetti, M. Hellström, Z. Hu, Z. Janas, R. Kirchner, F. Moroz, A. Piechaczek, A. Płochocki, E. Roeckl, B. Rubio, K. Rykaczewski, M. Shibata, J. Szerypo, J.L. Tain, V. Wittmann, A. Wöhr, Nucl. Phys. A 690 (2001) 367.
[30] G. Audi, A.H. Wapstra, Nucl. Phys. A 565 (1991) 1.
[31] C. Mazzocchi, Z. Janas, L. Batist, V. Belleguic, J. Döring, M. Gierlik, M. Kapica, R. Kirchner, G.A. Lalazissis, H. Mahmud, E. Roeckl, P. Ring, K. Schmidt, P.J. Woods, J. Zylicz, Phys. Lett. B 532 (2002) 29.
[32] I. Mukha, E. Roeckl, J. Döring, L. Batist, A. Blazhev, H. Grawe, C.R. Hoffman, M. Huyse, Z. Janas, R. Kirchner, M. La Commara, C. Mazzocchi, C. Plettner, S.L. Tabor, P. Van Duppen, M. Wiedeking, Phys. Rev. Lett. 95 (2005) 022501-1.
[33] I. Mukha, E. Roeckl, J. Döring, L. Batist, A. Blazhev, H. Grawe, C.R. Hoffman, M. Huyse, Z. Janas, R. Kirchner, M. La Commara, C. Mazzocchi, C. Plettner, S.L. Tabor, P. Van Duppen, M. Wiedeking, Nature 439 (2006) 298.
[34] G. Audi, A.H. Wapstra, C. Thibault, Nucl. Phys. A 729 (2003) 337.
[35] M. Mukherjee, A. Kellerbauer, D. Beck, K. Blaum, G. Bollen, F. Carre, P. Delahaye, J. Dilling, S. George, C. Guénaut, F. Herfurth, A. Herlert, H.-J. Kluge, U. Köster, D. Lunney, S. Schwarz, L. Schweikhard, C. Yazidjian, Phys. Rev. Lett. 93 (2004) 150801-1.
[36] K. Blaum, G. Audi, D. Beck, G. Bollen, F. Herfurth, A. Kellerbauer, H.-J. Kluge, E. Sauvan, S. Schwarz, Phys. Rev. Lett. 91 (2003) 260801-1.
[37] D. Rodríguez, V.S. Kolhinen, G. Audi, J. Äystö, D. Beck, K. Blaum, G. Bollen, F. Herfurth, A. Jokinen, A. Kellerbauer, H.-J. Kluge, M. Oinonen, H. Schatz, E. Sauvan, S. Schwarz, Phys. Rev. Lett. 93 (2004) 161104-1.
[38] A. Kellerbauer, G. Audi, D. Beck, K. Blaum, G. Bollen, B.A. Brown, P. Delahaye, C. Guénaut, F. Herfurth, H.-J. Kluge, D. Lunney, S. Schwarz, L. Schweikhard, C. Yazidjian, Phys. Rev. Lett. 93 (2004) 072502-1.
[39] F. Herfurth, G. Audi, D. Beck, K. Blaum, G. Bollen, P. Delahaye, S. George, C. Guénaut, A. herlert, A. Kellerbauer, H.-J. Kluge, D. Lunney, M. Mukherjee, S. Rahaman, S. Schwarz, L. Schweikhard, C. Weber, C. Yazidjian, in: Proceedings of the 4th International Conference on Exotic Nuclei and Atomic Masses, Pine Mountain, USA, 12–16 September, Eur. Phys. J. A 25 (2005) s01, 17.
[40] A. Jokinen, T. Eronen, U. Hager, J. Hakala, S. Kopecky, A. Nieminen, S. Rinta-Antila, J. Äystö, Eur. Phys. J. A 25 (2005) s01, 27.